MICHIGAN STATE UNIVERSITY

CYCLOTRON LABORATORY

NUCLEAR STRUCTURE CALCULATIONS WITH REALISTIC TWO-BODY FORCES

S. MARIPUU

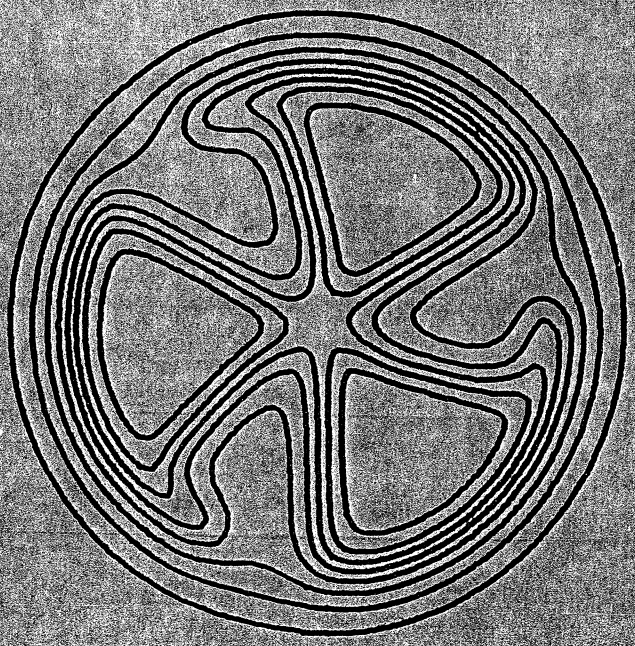

MSUCL – 70

OCTOBER 1972

Talk given at the "Fifth Symposium on Nuclear Structure of Low-Medium Mass Nuclei", 26-28 October, 1972, Lexington, Kentucky

Nuclear Structure Calculations with Realistic Two-body Forces

S. Maripuu

Cyclotron Laboratory, Dept. of Physics
Michigan State University
East Lansing, Michigan 48823, USA

I. INTRODUCTION

The promising results of the early work of Kuo and Brown[1-4] have inspired many studies of the use of realistic two-nucleon interactions in nuclear structure calculations. Realistic is used here to mean that the two-nucleon interaction is derived from the phase shift data from free nucleon-nucleon scattering. The two-nucleon interaction so derived is then transformed into an effective interaction to be used in a small model space. The successful results obtained by employing this method are many. A large number of physical quantities have been explained accurately, usually at least as well as is managed with empirical interactions (see e.g. Refs. 5 and 6). These latter interactions, deduced from energy spectra of simple nuclei or obtained as parameters from least squares fits to many energy levels often produce results which agree well with experimental data but their connections to the fundamental nucleon-nucleon problem are obscure. It has been shown that some matrix elements of empirically obtained two-body interaction are poorly determined by almost any feasible data set.[7]

An interesting alternative to the Kuo-Brown method for calculating realistic two-body interactions has been suggested by Elliott and his collaborators at Sussex.[8,9] They deduce relative harmonic oscillator matrix elements directly from the experimental scattering phase shifts without explicit construction of the potential. The method is a distorted wave Born approximation with reasonable (but not detailed) assumptions about the

smoothness and range of the potential. In spite of a number of applications with the Sussex matrix elements (see e.g. Ref. 10), they have rarely been used in detailed large space nuclear structure calculations.

The present calculations employ the Sussex matrix elements to derive effective interactions in the model space of a) the 0p-shell, b) the 0d-1s shell and c) the upper part of the 0d-1s shell including some 0f-1p excitations. The method of calculation is outlined in Section II and the different applications together with conclusions are presented in Sections III-V.

II. METHOD OF CALCULATION

The relative harmonic oscillator matrix elements given in Ref. 9 are used to calculate the present two-body matrix elements. The necessary transformation from jj to LS coupling as well as the Brody-Moshinsky transformation between the laboratory frame and the centre-of-mass and relative frame has been described by Kuo and Brown.[1] We have performed these transformations for different sets of b, the oscillator length parameter, which has been chosen to fit the nuclear size. The two-body matrix elements thus obtained are considered to correspond to the "bare" reaction matrix elements of Kuo and Brown. In order to be used in a small model space these matrix elements have to be corrected for space truncation effects. We have used perturbation theory (see e.g. Ref. 11) up to second order to calculate 3p-1h, 2h and 2p corrections. Energy denominators up to 2 $\hbar\omega$ excitations

have been included. The corrections are shown as diagrams in Fig. 1. The first diagram represents the unperturbed interaction, V. The energy denominators (expressed in units of $\hbar\omega$) always have the same oscillator size parameter, as the one used in the calculation of the unperturbed matrix elements. In other words, once the calculation starts, there are no free parameters in the two-body matrix elements.

We have taken the single-particle energies or one-body interactions from the spectra of closed-shell-plus-one nucleon nuclei. This approach has been commonly used in earlier investigations. In the calculations of energy spectra in nuclei far from the closed shells we have also treated the single-particle binding energy differences as free parameters (see Sec. III and V).

The construction of Hamiltonians and diagonalization of the energy matrices has been performed with the codes described by French, Halbert, McGrory, and Wong.[12]

III. STRUCTURE OF A=6-13 NUCLEI

We have calculated numerous properties of the 0p shell nuclei with the method described in Section II. The two-body matrix elements obtained for the 0p shell model space are listed in Table I. As seen from Table I, the perturbative corrections change the two-body matrix elements significantly. Furthermore, they are definitely needed if one is to obtain satisfactory agreement between experiment and theory. The effective matrix

elements shown in the last column of Table I are found to be similar to those determined from the least-squares fittings of Cohen and Kurath[13] and of Goldhammer and coworkers.[14] A detailed comparison, however, is not quite in order since the one-body parameters used by the above mentioned authors are different from ours.

Recent experimental data indicate (somewhat surprisingly) that all 0p nuclei have approximately the same rms radius.[15] Except for the absolute binding energies for different mass numbers (the accurate calculation of which we have not attempted), we find no significant changes in energy spectra for different values of the oscillator size parameter. We use therefore a fixed value, b=1.7 fm, for all nuclei. On the other hand, we have found a definite need to increase the energy separation between the $p_{3/2}$ and $p_{1/2}$ single particle states (ΔE) with increasing mass number. For A=6 we find ΔE=3 MeV (the experimental spin-orbit splitting as observed in A=5 is 2.6 ± 0.4 MeV), and for A=13 we have adopted ΔE=7 MeV.

Experimental and calculated energy spectra for A=6-8 and A=11-13 nuclei are shown in Figs. 2 and 3, respectively. The results are encouraging, and perhaps much better than one might expect for a one parameter theory. We notice two minor discrepancies between the theoretical and experimental spectra.

1. The three lowest levels in ^{8}Be are calculated about 2 MeV too high (in comparison with other levels of the ^{8}Be spectrum). Also, the 7.7 and 10.1 MeV levels in ^{12}C are predicted to be higher than the experimental energies.

2. The lowest J^π $T=0^+1$ states in A=6, 10 and 14 are predicted about 2 MeV too low.

The first discrepancy is easy to understand. The five experimental states involved have large reduced α particle widths, indicating deformed α-particle type structures.[16] For an accurate description of these states in the shell model, we would need a larger configuration basis. The second discrepancy could possibly be rectified by including higher order corrections into the perturbation calculation (or by including a monopole shift to increase the isospin splitting[17]).

With the wave functions obtained for a number of different ΔE values, we have calculated magnetic dipole moments, M1 transition strengths, log ft values for β-decay and single nucleon spectroscopic factors. In Figs. 4 and 5 we show how the calculated magnetic dipole moments vary with ΔE. In most cases the experimental and theoretical values coincide for reasonable ΔE values. Furthermore, it appears that for T=0 states the predicted magnetic moments are very insensitive to the variation of ΔE (or, in other words, to the amount of configuration mixing). This is due to the following reasons:

(i) The isoscalar reduced single nucleon matrix element $\langle p_{3/2}||\mu_{IS}||p_{3/2}\rangle$ is about five times larger than the $\langle p_{3/2}||\mu_{IS}||p_{1/2}\rangle$ and $\langle p_{1/2}||\mu_{IS}||p_{1/2}\rangle$ matrix elements.

(ii) In almost all many-nucleon configurations of the 0p shell there is at least one $p_{3/2}$ nucleon. All diagonal matrix elements will therefore be of about the same size (roughly the size of the matrix element $\langle p_{3/2}||\mu_{IS}||p_{3/2}\rangle$).

We thus conclude that to a good approximation, configuration mixing does not affect the total isoscalar matrix elements. (This is not true for the isovector matrix elements because there the off-diagonal single-nucleon reduced matrix elements are comparatively large).

Various quantities connecting the $J^{\pi}=1/2^{-}$ and $3/2^{-}$ ground and first-excited states of A=13 are shown in Fig. 6. Again, the variation of the predicted values with ΔE is included. Most observables are predicted best at $\Delta E \approx 6.8$ MeV, but the β-decay rates favor a value of $\Delta E \approx 5.0$ MeV. This comparatively retarded β-decay might be explained with sd-shell admixtures in the ^{13}B ground state.

From a detailed comparison of various calculated quantities we conclude that our calculations yield about the same results as those obtained in previous calculations with many parameters[13,14] (our energy level predictions are not quite as good). Therefore, we find it encouraging that a calculation, essentially without parameters and derived from first principles does as well as those with effective two-body matrix elements obtained from least-squares fits with upwards of thirteen free parameters.

IV. ENERGY LEVELS OF A=18-22 NUCLEI

Excitation energies in A=18-22 nuclei have been calculated in full 0s1d model space. The calculation of the effective two-body interaction has, in principle, already been described in the previous sections. Again, perturbative corrections up to second order and to 2 $\hbar\omega$ excitations have been included. For A=18-22 nuclei we have used the same harmonic oscillator size parameter, $\hbar\omega$=14.4 MeV, as in the A=6-13 calculation. The single-particle energies have been taken from the ^{17}O experimental spectrum. The absolute ground state binding energies calculated in this way turn out to be somewhat too large (interaction too attractive), indicating that better agreement would have been obtained with a somewhat smaller oscillator constant. (The absolute binding energies of the lowest T states in A=19 and 22 are predicted about 0.5 and 4.0 MeV too low, respectively).

The spectra of ^{18}F and ^{18}O are shown in Figs. 7 and 8. The energy scales used in Figs. 7 and 8 indicate binding energy with respect to ^{16}O. The agreement between experiment and theory is good except for the J^π T=1$^+$0 ground state of ^{18}F which is predicted somewhat too high. The calculated and experimental spectra of ^{19}F, ^{20}Ne, ^{20}F and ^{20}O, all with ground state energies set equal are shown in Figs. 9-12. The agreement between experimental and calculated excitation energies is again quite good. The calculated spectra are very similar to those obtained with the Kuo-Brown interaction.[5,6] A comparison is shown only

for the ^{20}O spectrum in Fig. 12. (The Kuo-Brown two-body matrix elements contained some small errors,[18] therefore a detailed comparison has been left out). In all spectra shown in Figs. 7-12, the energy levels drawn with somewhat heavier lines indicate levels presumably belonging to the ground-state bands. It is experimentally well established[19] that the second $7/2^+$ state in ^{19}F (see Fig. 9) belongs to the ground state band. Our calculation, however, predicts a fairly complicated $7/2^+$ state as the lowest state (and the second $7/2^+$ as predominantly of $d^3_{5/2}$ character).

It is well-known that realistic interactions do not produce enough splitting between groups of energy levels with different isospin. In Fig. 13 we have plotted the ground state binding energies for A=19-22 nuclei. For each mass number we have normalized the spectrum to the binding energy of the ground state with lowest isospin. Included are also some levels close to the experimental (or predicted) ground states. For A=22, we did not calculate the $J^\pi T=3^+0$ level, the calculated energies are normalized to the lowest experimental $J^\pi T=1^+0$ level. It can be concluded from Fig. 13 that for most cases the predicted isospin splitting is only slightly smaller than the observed one. Larger discrepancies are found for the newly measured binding energies of ^{21}O and ^{22}O.[20]

We find that the inclusion of the 2p-corrections greatly improves the isospin splitting. Inclusion of higher order

corrections might remove the remaining discrepancies provided the present model space is reasonable. As already mentioned, a smaller oscillator size would predict better absolute binding energies. However, it is not clear whether a physically reasonable size parameter will accomplish such an agreement.

V. CONFIGURATION MIXING OF THE df AND dp MULTIPLETS OF ^{38}Cl

The early description of the low-lying negative-parity quartets of ^{38}Cl and ^{40}K[21,22] has led to the consideration of these states as members of relatively pure $(\pi d_{3/2}\nu f_{7/2})$ and $(\pi d_{3/2}^{-1}\nu f_{7/2})$ configurations, respectively, with the spectra of the two nuclei almost perfectly related by the particle-hole transformation. More recent measurements[23,24] have revealed a higher lying multiplet with the $1p_{3/2}$ neutron replacing the $0f_{7/2}$ neutron, although the transformation of energies is not as accurate for this multiplet as for the lower set of states.

However, measurements on M1 strengths in ^{38}Cl[24-26] cast serious doubt on this simple description of these states. A strong M1 transition is observed from the 3^- state of the dp-multiplet to the 4^- state of the df-multiplet. This transition is, of course, ℓ-forbidden to the extent that the wave functions of the states actually are made of such configurations. Other data that contradict the pure configuration picture are the spectroscopic factors for the ^{37}Cl(d,p)^{38}Cl reaction.[27] These experiments show some ℓ=1 admixing into the 3^- state of the lower multiplet.

We have calculated excitation energies, M1 transition strengths and single nucleon spectroscopic factors for A=38-40 nuclei in a model space which includes active $d_{5/2}$, $s_{1/2}$, $d_{3/2}$, $f_{7/2}$ and $p_{3/2}$ particles.* The relative single-particle energies were chosen to yield calculated spectra for ^{38}Cl, ^{39}K and ^{40}K in simultaneous best agreement with the experimental spectra. We found the values -9.40, -4.90, -2.67, -2.52 and 0.00 MeV for the $d_{5/2}$, $s_{1/2}$, $d_{3/2}$, $f_{7/2}$ and $p_{3/2}$, respectively. Our calculated M1 transitions strength for ^{38}Cl are summarized in Fig. 14 and Table II. The ^{40}K M1 transitions are also included in Table II. The calculated spectroscopic factors are compared with the experimental ones in Fig. 15. Our predictions for these observables (our M1 calculations use operators calculated from the bare nucleon g-factors) are in uniform good agreement with the observed values. In particular, for ^{38}Cl, the mixing of the ℓ=1 and ℓ=3 strengths for the 3^- states and, most striking, the anomalously large $3^-_2 \to 4^-$ M1 transition are correctly predicted.

The difficulty of accounting for this M1 transition, enhanced when it should be severely retarded according to simple ideas, has been frequently noted of late.[28,29] No previous calculation has been able to reproduce the observed strength. It is therefore of interest to see how the correct strength emerges from the present wave functions. (In Table III we have listed the intensities of different configurations in our model space for ^{38}Cl and ^{40}K). The components in the wave functions of the 3^-_2

---

* The method of calculation of the two-body interaction is the same as the one described in previous sections. The size parameter, $\hbar\omega$, has been chosen to be 12.8 MeV.

and 4_1^- state which are important contributors to this strength are given in Table IV.* Also included in Table IV are the important contributions for the $3_2^- \rightarrow 3_1^-$ M1 transition. We see that the excitations from the $s_{1/2}$ to the $d_{3/2}$ orbit are of comparable importance to the mixing between $f_{7/2}$ and $p_{3/2}$ excitations in contributing to the M1 transition strength. (The $s_{1/2}$ particles, as well as $f_{7/2}$ and $p_{3/2}$, have their spins parallel to the orbital angular momentum, thus producing strong isovector contributions to the M1 strength[30]). Furthermore, it is important to notice that the strong contributions to the $3_2^- \rightarrow 4^-$ transition add up coherently. The individual contributions to the $3_2^- \rightarrow 3_1^-$ are even larger than those for the $3_2^- \rightarrow 4^-$ transition (as pointed out by Erné et al.[31]). However, in this case the signs of the individual components are such that the various contributions cancel each other.

We arrive at the following conclusions:

(i) the df and dp multiplets in ^{38}Cl are about 80% pure, with considerable mixing only between the 3^- states.

(ii) The 5%-20% admixtures of the $s_{1/2}^{-1}$ configurations in these ^{38}Cl states are important to account for the $3_2^- \rightarrow 4^-$ anomalous M1 strength.

(iii) The purity of the $d^{-1}f$ and $d^{-1}p$ multiplets in ^{40}K is considerably higher (no anomalies in M1 strength are predicted) in agreement with observations. The differences between ^{38}Cl and ^{40}K are consequences of the freedom to excite particles within the sd-shell which exists for ^{38}Cl but does not exist for ^{40}K.

---

* Only isovector components have been included since no large isoscalar contributions have been predicted.

ACKNOWLEDGEMENTS

This talk describes work carried out by A.O. Evwaraye, Gale I. Harris, Paul S. Hauge, B.H. Wildenthal and myself.

Part of this investigation was initiated at the Aerospace Research Laboratories under a NRC-AFLC contract. It has been partly supported by the National Science Foundation.

REFERENCES

1. T.T.S. Kuo and G.E. Brown, Nucl. Phys. 85, 40(1966).
2. T.T.S. Kuo, Nucl. Phys. A103, 71(1967).
3. G.E. Brown and T.T. S. Kuo, Nucl. Phys. A92, 481(1967).
4. T.T.S. Kuo and G.E. Brown, Nucl. Phys. A114, 241(1968).
5. E.C. Halbert, in The Structure of Low-Medium Mass Nuclei, edited by J.P. Davidson (University of Kansas Press, Lawrence, Kansas, 1968), p. 128.
6. E.C. Halbert, J.B. McGrory, B.H. Wildenthal and S.P. Pandya, Advances in Nuclear Physics, Vol. 3 edited by M. Baranger and E. Vogt (Plenum Press, New York, 1969).
7. M.H. Macfarlane, in The Two-Body Force in Nuclei, edited by S.M. Austin and G.M. Crawley (Plenum Press, New York-London, 1972), p. 1.
8. J.P. Elliott, in The Structure of Low-Medium Mass Nuclei, edited by J.P. Davidson (University of Kansas Press, Lawrence, Kansas, 1968), p. 48.
9. J.P. Elliott, A.D. Jackson, H.A. Mavromatis, E.A. Sanderson and B. Singh, Nucl. Phys. A121, 241(1968).
10. B.S. Cooper, J.B. Seaborn and S.A. Williams, Phys. Rev. C4, 1997(1971).
11. T.T.S. Kuo, Nucl. Phys. A90, 199(1967).
12. J.B. French, E.C. Halbert, J.B. McGrory and S.S.M. Wong, Advances in Nuclear Physics, Vol. 2 (Plenum Press, New York, 1970) p. 193.
13. S. Cohen and D. Kurath, Nucl. Phys. 73, 1(1965).

14. P. Goldhammer, J.R. Hill and J. Nachamkin, Nucl. Phys. A106, 62(1968); J.L. Norton and P. Goldhammer, Nucl. Phys. A165, 33(1971).

15. D.H. Wilkinson and M.E. Mafethe, Nucl. Phys. 85, 97(1966).

16. T. Kanellopoulos and K. Wildermuth, Nucl. Phys. 14, 349(1960); H. Morinaga, Phys. Lett. 21, 78(1966).

17. M. Dworzecka and H. McManus, Bull. Amer. Phys. Soc. 17, 554(1972).

18. T.T.S. Kuo, in The Structure of Low-Medium Mass Nuclei, edited by J.P. Davidson (University Press of Kansas, Lawrence, Kansas, 1972), p. 75.

19. H.G. Bingham and H.T. Fortune, Bull. Am. Phys. Soc. Vol. 3, No. 19, 20(1972).

20. A.G. Artukh et al., Nucl. Phys. A192, 170(1972).

21. S. Goldstein and I. Talmi, Phys. Rev. 102, 589(1956).

22. S.P. Pandya, Phys. Rev. 103, 956(1956).

23. R.M. Freeman and A. Gallman, Nucl. Phys. A156, 305(1970).

24. G.A.P. Engelbertink and J.W. Olness, Phys. Rev. C5, 431(1972).

25. R.E. Segel et al., Phys. Rev. Lett. 25, 1352(1970) and to be published.

26. R. Bass and R. Wechsung, Phys. Lett. 32B, 602(1970).

27. J. Rapaport and W.W. Buechner, Nucl. Phys. 83, 80(1966).

28. D. Kurath and R.D. Lawson, Phys. Rev. C6, 901(1972).

29. P. Goode, Bull. Am. Phys. Soc. 17, 34(1972) and to be published.

30. S. Maripuu, Nucl. Phys. A123, 357(1967).

31. F. Erne, W.A.M. Veltman and J.A.J.M. Wintermans, Nucl. Phys. 88, 1(1966).

TABLE I

The Two-Body Matrix Elements in the form $\langle ab;JT|V|cd;JT\rangle$, are shown for the 0p shell along with their perturbative corrections. The numbers abcd represent $2J_a$, $2J_b$, $2J_c$, and $2J_d$ respectively. All matrix elements are calculated for the length parameter b=1.7 fm and expressed in MeV.

a b c d - J T	$\langle V\rangle$	$\langle V_{3p-1h}\rangle$	$\langle V_{4p-2h}\rangle$	$\langle V_{2p}\rangle$	$\langle V_{eff}\rangle$
3 3 3 3 - 1 0	-1.541	-0.055	-0.112	-0.838	-2.546
- 3 0	-4.060	-0.158	-	-0.764	-4.982
- 0 1	-3.020	-0.276	-0.303	-0.414	-4.013
- 2 1	-1.453	+0.314	-	-0.170	-1.308
3 3 3 1 - 1 0	+3.528	+0.059	+0.316	+0.562	+4.465
- 2 1	-1.539	-0.276	-	-0.127	-1.942
3 3 1 1 - 1 0	+1.676	+0.026	-0.138	+0.437	+2.001
- 0 1	-3.606	-0.643	-0.214	-0.176	-4.639
3 1 3 1 - 1 0	-4.770	+0.196	-0.888	-0.923	-6.385
- 2 0	-5.350	+0.156	-	-1.255	-6.449
- 1 1	-0.728	+0.544	-	-0.051	-0.235
- 2 1	-2.542	+0.522	-	-0.261	-2.281
3 1 1 1 - 1 0	+0.942	+0.256	+0.389	-0.174	+1.413
1 1 1 1 - 1 0	-1.843	+0.065	-0.170	-0.722	-2.670
- 0 1	-0.470	+0.264	-0.152	-0.289	-0.647

TABLE II

M1 Transitions in ^{38}Cl and ^{40}K

^{38}Cl				^{40}K			
	M1 Strength (W.U.)				M1 Strength (W.U.)		
$J_i \to J_f$	Argonne[25]	Brookhaven[24]	Theory	$J_i \to J_f$	Argonne[25]	Frankfurt[26]	Theory
$3_1^- \to 2_1^-$	.23	.13	.10	$3_1^- \to 4^-$	.150	.170	.087
$4^- \to 3_1^-$	.062	.034	.029	$2_1^- \to 3_1^-$	.127	.140	.091
$4^- \to 5^-$	.170	.091	.074	$5^- \to 4^-$	.030	.030	.027
$3_2^- \to 4^-$	.38	.24	.20	$2_2^- \to 2_1^-$	.0130	.0100	.0045
$3_2^- \to 3_2^-$	.0084	.0054	.0069	$2_2^- \to 3_2^-$	.0026	.0023	.0016
$3_2^- \to 2_1^-$	.00105	.00070	.00044	$3_2^- \to 2_1^-$	.0033	.0020	.0048
$1^- \to 2_1^-$	.0050	.0031	.0036	$3_2^- \to 3_1^-$	.0046	.0025	.0053
$2_2^- \to 3_1^-$	.0174	.0098	.0057	$3_2^- \to 4^-$	.0030	.0016	.0012
$2_2^- \to 2_1^-$	.0053	.0030	.0065	$1^- \to 2_1^-$	.0076	.0038	.0222
$2_2^- \to 1^-$	.62	.36	.45	$0^- \to 1^-$	.47	.20	.91
$2_2^- \to 3_2^-$	.80	.46	.31				

TABLE III

Configuration Mixing in ^{38}Cl and ^{40}K
(intensities in %)

^{38}Cl	E_x(MeV)		J^π	$d^5_{3/2}f_{7/2}$	$d^5_{3/2}p_{3/2}$	$s^{-1}_{1/2}d^6_{3/2}f_{7/2}$	$s^{-1}_{1/2}d^6_{3/2}p_{3/2}$
	Exp	Calc					
	0	0	2^-	82	3	7	2
	.67	.39	5^-	86		5	
	.76	.63	3^-	68	17	7	2
	1.31	1.34	4^-	77		8	
	1.62	1.49	3^-	14	45	28	1
	1.69	2.11	1^-		81	12	3
	1.75	1.51	0^-		97		1
	1.98	1.92	2^-	1	77	16	1

^{40}K	E_x(MeV)		J^π	$d^{-1}_{3/2}f_{7/2}$	$d^{-1}_{3/2}p_{3/2}$	$s^{-1}_{1/2}f_{7/2}$	$s^{-1}_{1/2}p_{3/2}$
	Exp	Calc					
	0	0	4^-	96		2	
	.03	-.02	3^-	91	5	2	
	.80	1.06	2^-	87	7		2
	.89	.79	5^-	96			
	2.05	1.99	2^-	6	89		
	2.07	1.93	3^-	2	76	18	
	2.10	2.54	1^-		96		
	2.63	2.19	0^-		98		

TABLE IV

Predominant contributions to the $J^{\pi}=3_2^- \rightarrow 4^-$ and $3_2^- \rightarrow 3_1^-$ M1 transitions strengths in ^{38}Cl. Initial and final configurations are the same. The configuration amplitudes are denoted α_i and α_f, respectively. The isovector matrix elements are expressed in nuclear magnetons.

Initial and Final Configuration	α_i	α_f	Pure IV-comp	Mixed IV-comp	Predominant Contribution
$3_2^- \rightarrow 4^-$					
$(d^5_{3/2})_{3/2,3/2} f_{7/2}$	-.37	-.87	-3.94	-1.28	$f_{7/2}$
$s^{-1}_{1/2}(d^6_{3/2})_{21} f_{7/2}$	-.39	-.13	-13.2	- .67	$s_{1/2}+f_{7/2}$
$s^{-1}_{1/2}(d^6_{3/2})_{01} f_{7/2}$	+.33	+.25	-15.4	-1.29	$s_{1/2}+f_{7/2}$
			TOTAL	-4.43	
$3_2^- \rightarrow 3_1^-$					
$(d^5_{3/2})_{3/2,3/2} f_{7/2}$	-.37	+.83	+13.5	-4.13	$f_{7/2}$
$(d^5_{3/2})_{3/2,3/2} p_{3/2}$	+.67	+.42	+13.8	+3.86	$p_{3/2}$
$s^{-1}_{1/2}(d^6_{3/2})_{01} f_{7/2}$	+.33	+.21	+22.4	+1.52	$s_{1/2}+f_{7/2}$
			TOTAL	+ .69	

FIGURE CAPTIONS

Fig. 1 The diagrams representing the perturbative corrections to the unperturbed interaction, V.

Fig. 2 Magnetic dipole moments of A=6-9 nuclei. Solid lines indicate experimental values. The dashed lines show how the predicted values vary with the $p_{3/2}$ and $p_{1/2}$ single particle energy difference.

Fig. 3 Magnetic moments of A=10-13 nuclei. See caption for Fig. 2.

Fig. 4 Comparison between theory and experiment for several quantities in A=13. Reading from top to bottom they are: The excitation energy of the first excited $3/2^-$ state in ^{13}C(and ^{13}N); the magnetic moments of the ^{13}C and ^{13}N ground states; the M1 transition strength from the 3.51 MeV, $J^\pi=3/2^-$ state in ^{13}N to the ground state; the ratio of the single nucleon spectroscopic factors between the ground state and first excited state of ^{13}C; the log ft values for $^{13}B \rightarrow {}^{13}C(1/2^-)$ and $^{13}B \rightarrow {}^{13}C(3/2^-)$ beta decays. The horizontal solid lines show measured values, with the thickness of the line indicating experimental uncertainties. The dashed lines show how the predicted values vary with the spin-orbit splitting, $\Delta E(p_{3/2}-p_{1/2})$. See also text.

Fig. 5 Experimental and calculated energy spectra for A=6-8 nuclei, all calculated with $\Delta E(p_{3/2}-p_{1/2})=3.0$ MeV.

Fig. 6 Experimental and calculated energy spectra for A=11-13 nuclei, all calculated with $\Delta E(p_{3/2}-p_{1/2})=7.0$ MeV.

Fig. 7 The T=0 spectrum of ^{18}F as observed experimentally and as calculated with the present interaction.

Fig. 8 The experimental and calculated spectrum of ^{18}O.

Fig. 9 Observed and predicted spectrum of ^{19}F.

Fig. 10 Observed and predicted spectrum of ^{20}Ne.

Fig. 11 Observed and predicted spectrum of ^{20}F.

Fig. 12 Observed spectrum for ^{20}O and shell-model spectra calculated with the present method and as calculated by Kuo (Ref. 6).

Fig. 13 Binding energies of ground states and a few other levels in A=19-22 nuclei. For each mass number the spectra have been normalized to the level with the lowest binding energy. (The experimentally observed energy-separations between different isobars have been adjusted by subtracting Coulomb-energy differences estimated as explained in Ref. 6). For ^{22}Ne the $J^{\pi}T=3^{+}0$ level has not been calculated, the predicted spectrum has been normalized to the lowest $J^{\pi}T=1^{+}0$ state.

Fig. 14 The excitation energies and M1 transition strengths of ^{38}Cl. Predicted quantities are shown within brackets.

Fig. 15 Single-nucleon spectroscopic factors for the $^{37}Cl(d,p)^{38}Cl$ reaction. For each level the experimental number is represented by the left hand bar; the bar immediately to its right is the calculated one.

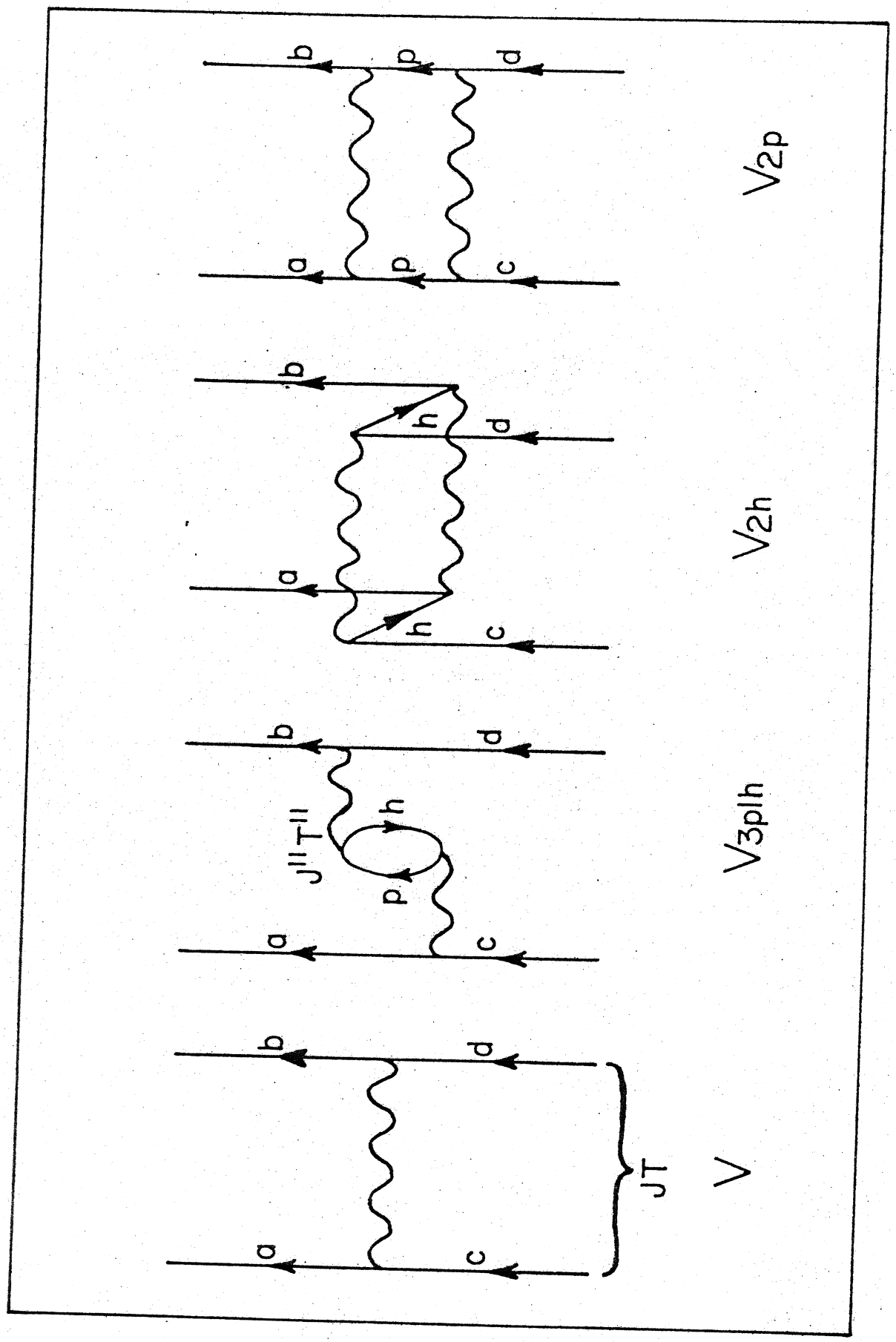

Fig. 1

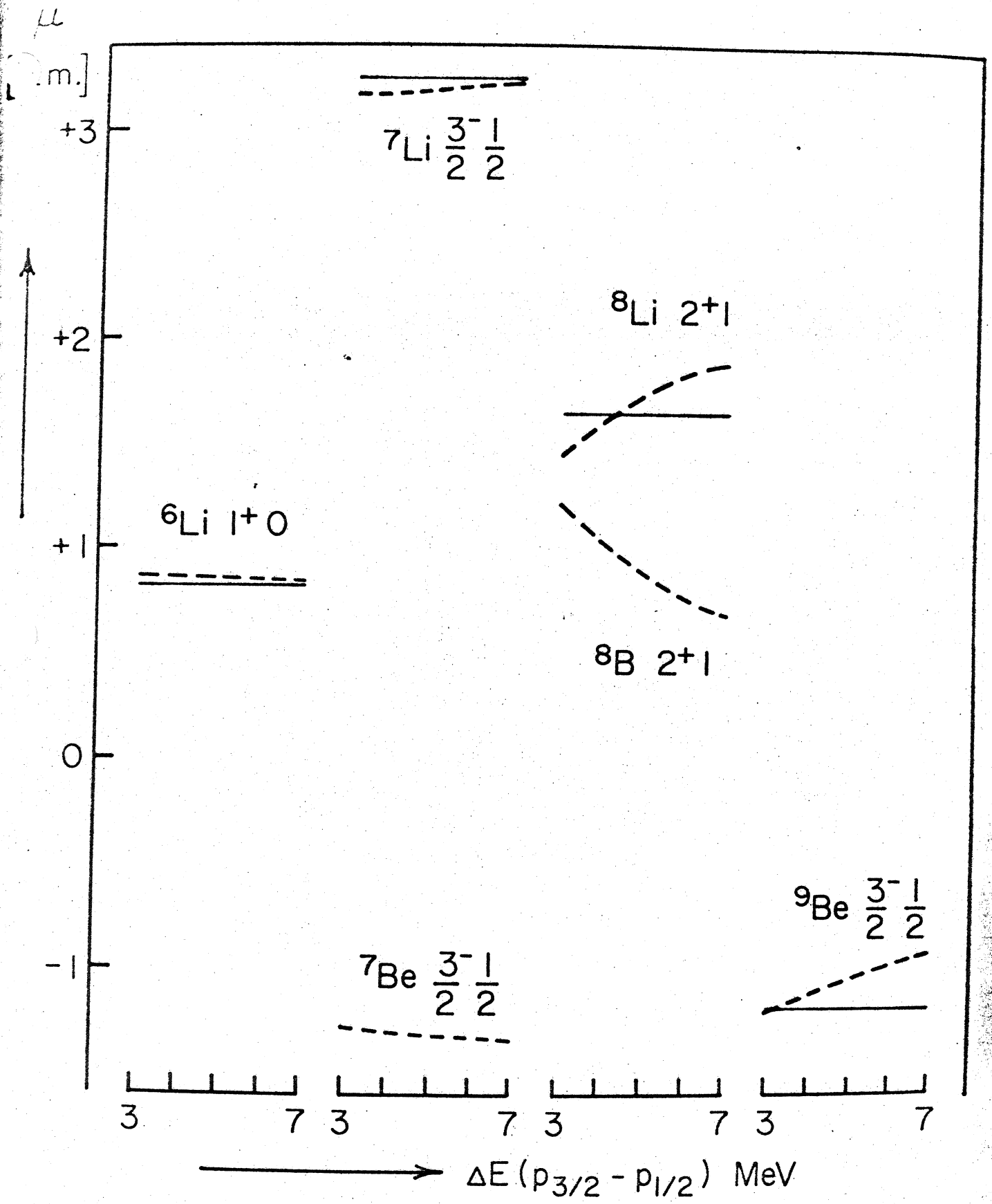
μ
[.m.]
+3
+2
+1
0
-1
^{7}Li $\frac{3^-}{2}\frac{1}{2}$
^{8}Li 2^+1
^{6}Li 1^+0
^{8}B 2^+1
^{9}Be $\frac{3^-}{2}\frac{1}{2}$
^{7}Be $\frac{3^-}{2}\frac{1}{2}$
3
7
3
7
3
7
3
7
$\Delta E (p_{3/2} - p_{1/2})$ MeV

Fig. 2

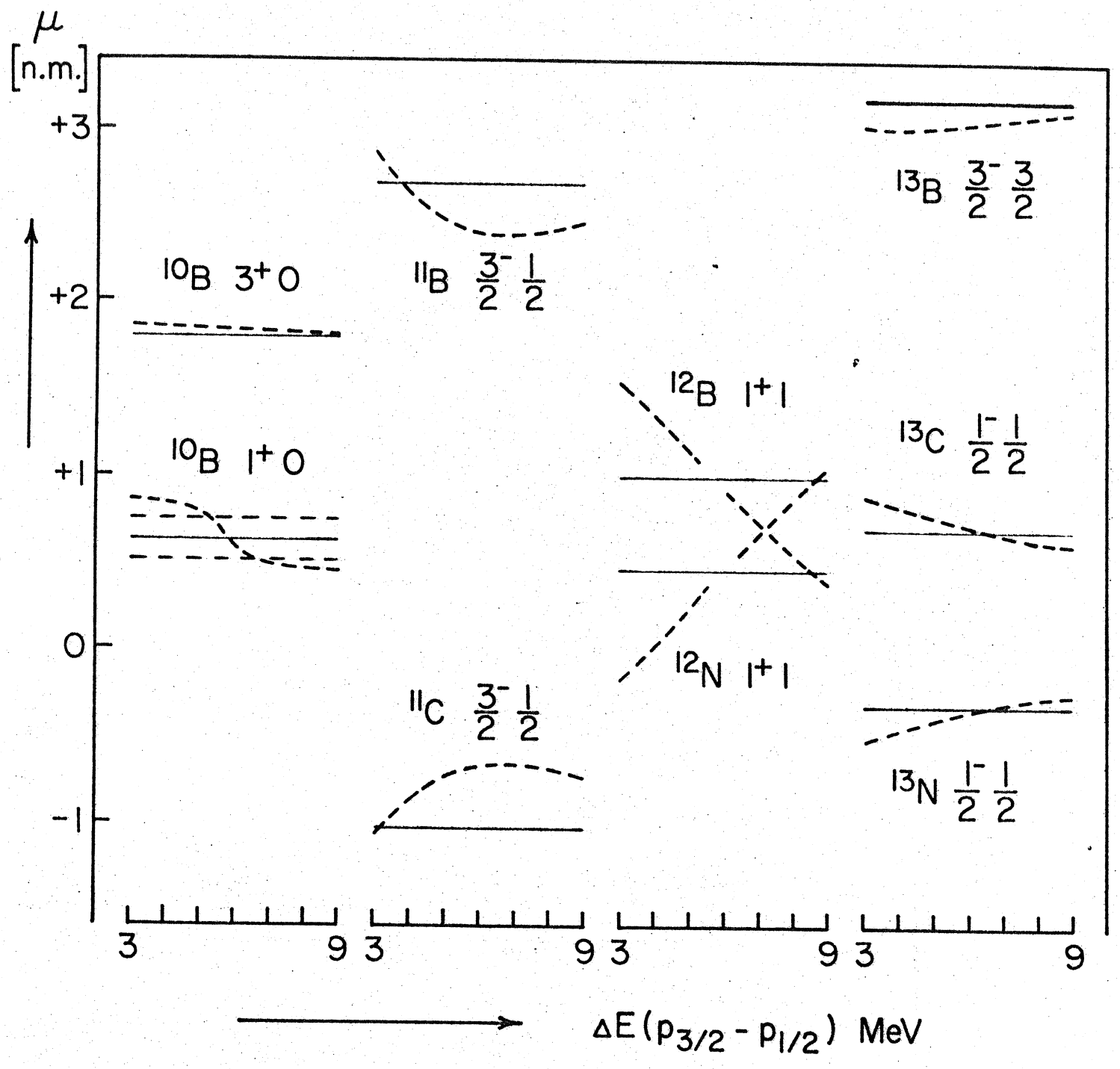
μ
[n.m.]
+3
+2
+1
0
-1
10B 3+ 0
10B 1+ 0
11B 3/2- 1/2
11C 3/2- 1/2
12B 1+ 1
12N 1+ 1
13B 3/2- 3/2
13C 1/2- 1/2
13N 1/2- 1/2
3
9
3
9
3
9
3
9
ΔE (p3/2 - p1/2) MeV

Fig. 3

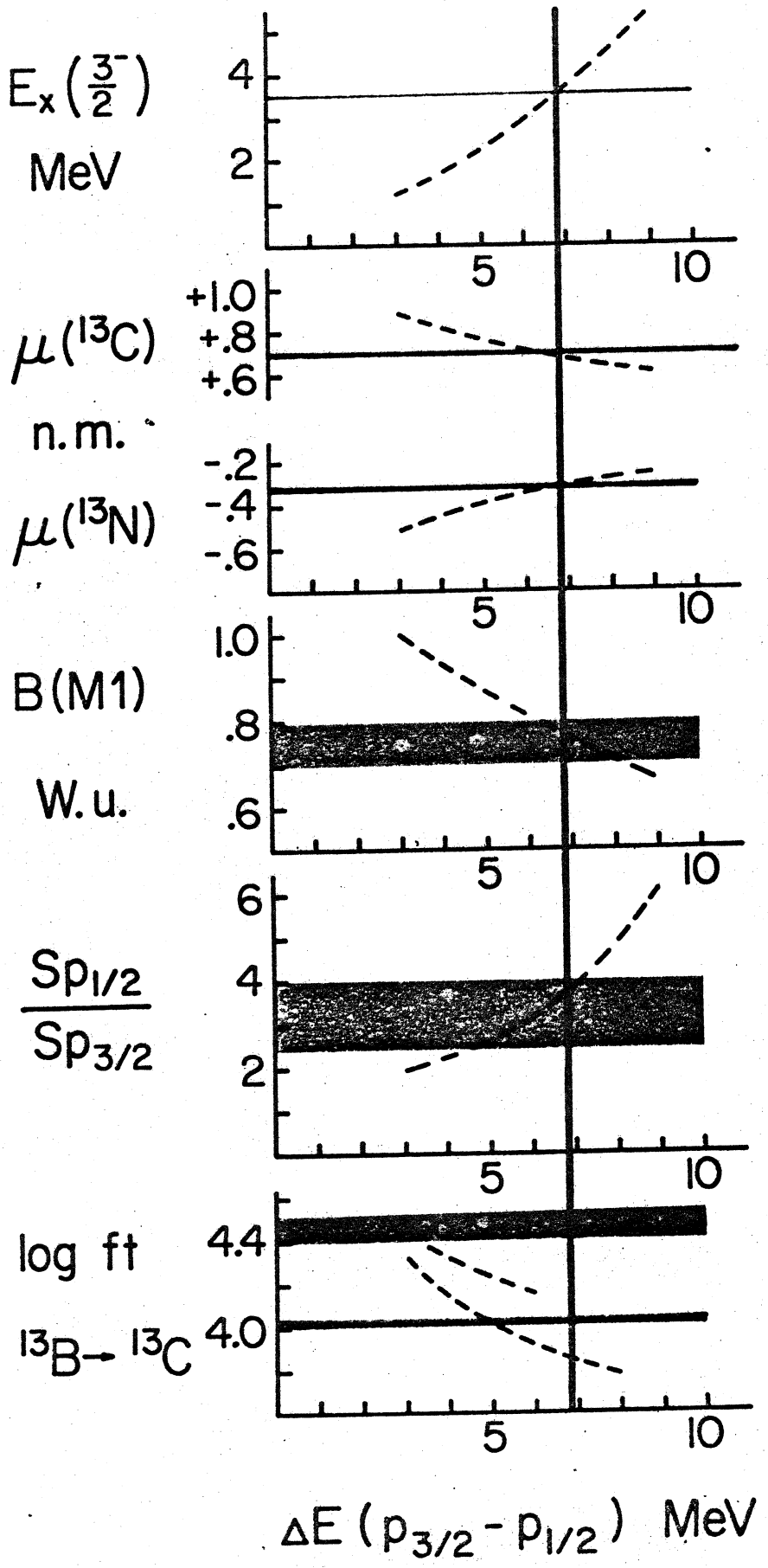
$E_x(\frac{3^-}{2})$
MeV
4
2
5
10
$\mu(^{13}C)$
n.m.
+1.0
+.8
+.6
$\mu(^{13}N)$
-.2
-.4
-.6
5
10
B(M1)
W.u.
1.0
.8
.6
5
10
$\frac{Sp_{1/2}}{Sp_{3/2}}$
6
4
2
5
10
log ft
$^{13}B \rightarrow {}^{13}C$
4.4
4.0
5
10
$\Delta E\,(p_{3/2} - p_{1/2})$ MeV

Fig. 4

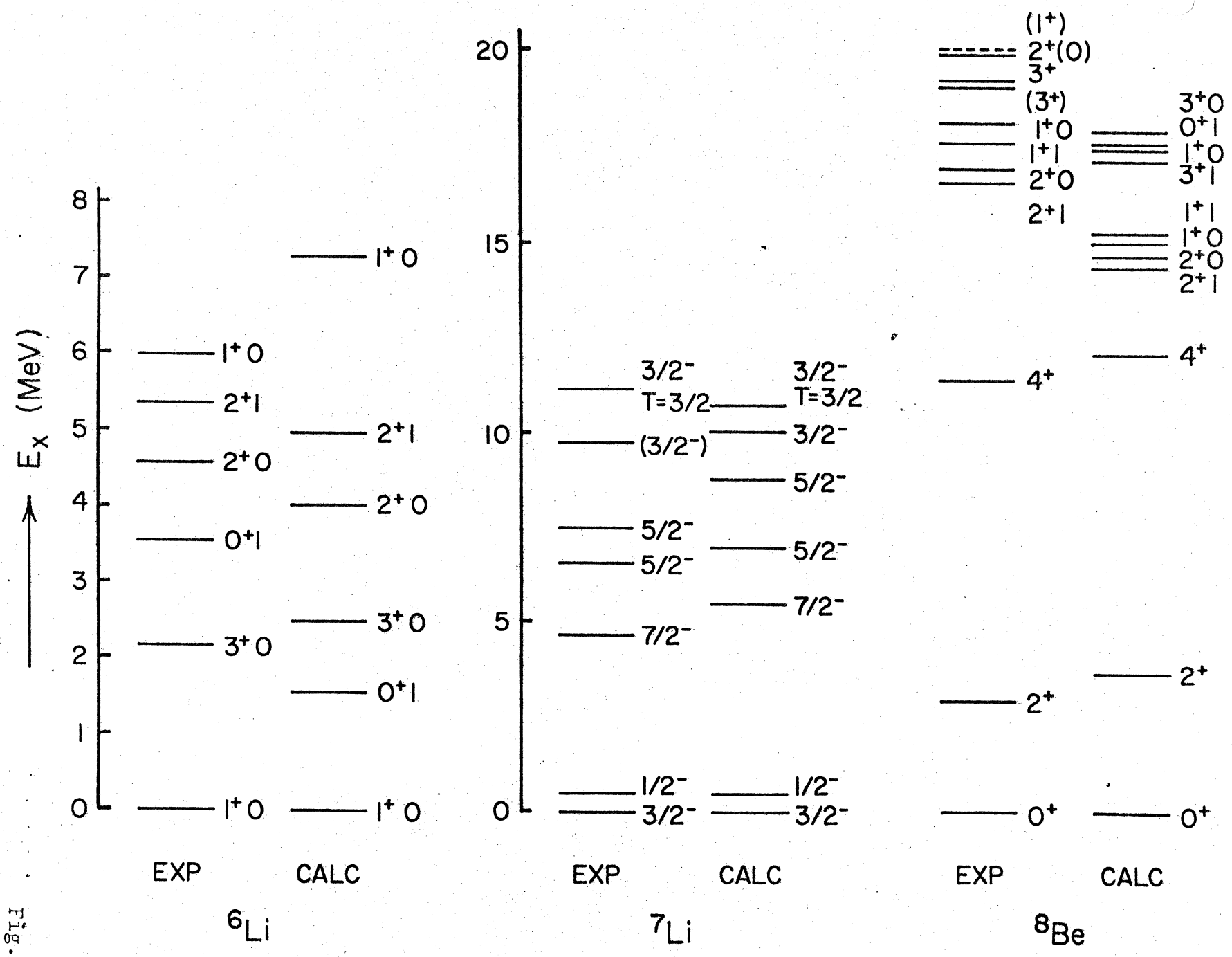
E_x (MeV)
0
1
2
3
4
5
6
7
8
1^+0
2^+1
2^+0
0^+1
3^+0
1^+0
1^+0
2^+1
2^+0
3^+0
0^+1
1^+0
EXP
CALC
^{6}Li
0
5
10
15
20
$1/2^-$
$3/2^-$
$7/2^-$
$5/2^-$
$5/2^-$
$(3/2^-)$
$3/2^-$ T=3/2
$1/2^-$
$3/2^-$
$7/2^-$
$5/2^-$
$5/2^-$
$3/2^-$
$3/2^-$ T=3/2
EXP
CALC
^{7}Li
0^+
2^+
4^+
2^+1
2^+0
1^+0
3^+
$2^+(0)$
(1^+)
0^+
2^+
4^+
3^+1
1^+0
0^+1
3^+0
2^+1
2^+0
1^+0
1^+1
EXP
CALC
^{8}Be

Fig. 5

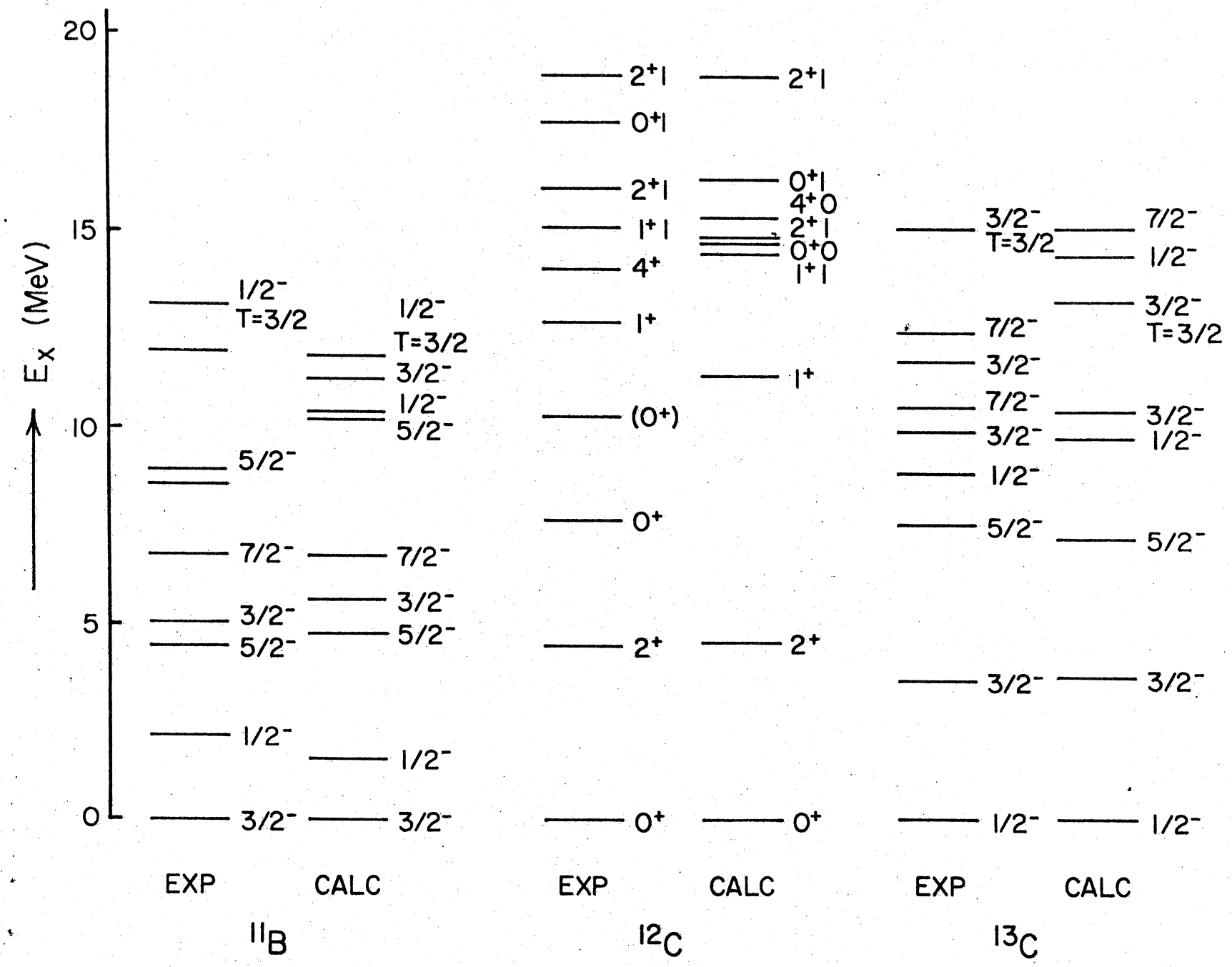
20
15
10
5
0
E_x (MeV)
1/2⁻ T=3/2
5/2⁻
7/2⁻
3/2⁻
5/2⁻
1/2⁻
3/2⁻
1/2⁻ T=3/2
3/2⁻
1/2⁻
5/2⁻
7/2⁻
3/2⁻
5/2⁻
1/2⁻
3/2⁻
EXP
CALC
^{11}B
2⁺1
0⁺1
2⁺1
1⁺1
4⁺
1⁺
(0⁺)
0⁺
2⁺
0⁺
2⁺1
0⁺1
4⁺0
2⁺1
0⁺0
1⁺1
1⁺
2⁺
0⁺
EXP
CALC
^{12}C
3/2⁻ T=3/2
7/2⁻
3/2⁻
7/2⁻
3/2⁻
1/2⁻
5/2⁻
3/2⁻
1/2⁻
7/2⁻ T=3/2
1/2⁻
3/2⁻ T=3/2
3/2⁻
1/2⁻
5/2⁻
3/2⁻
1/2⁻
EXP
CALC
^{13}C

Fig. 6

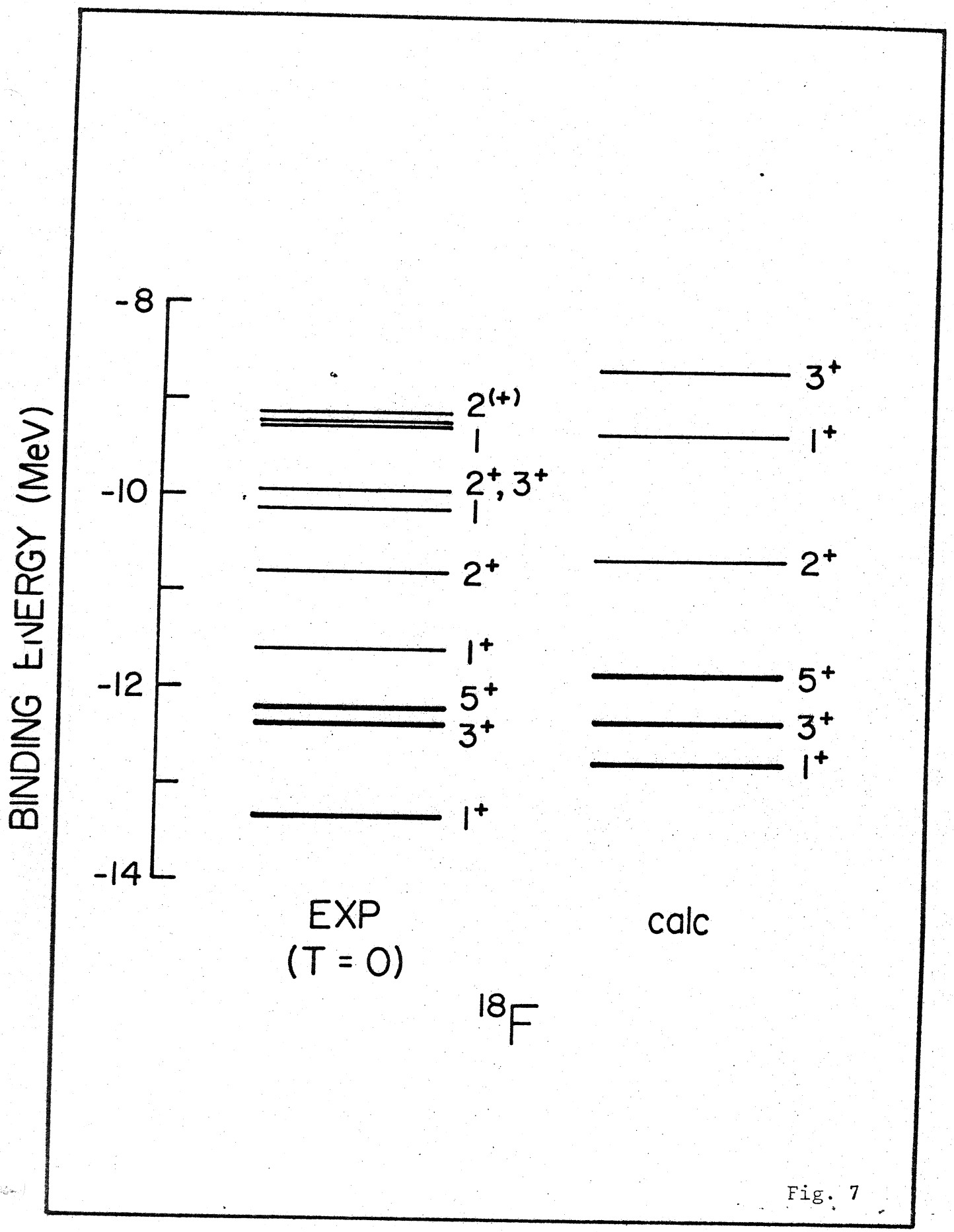
BINDING ENERGY (MeV)
-8
-10
-12
-14
2(+)
1
2+, 3+
1
2+
1+
5+
3+
1+
3+
1+
2+
5+
3+
1+
EXP
(T = 0)
calc
18F

Fig. 7

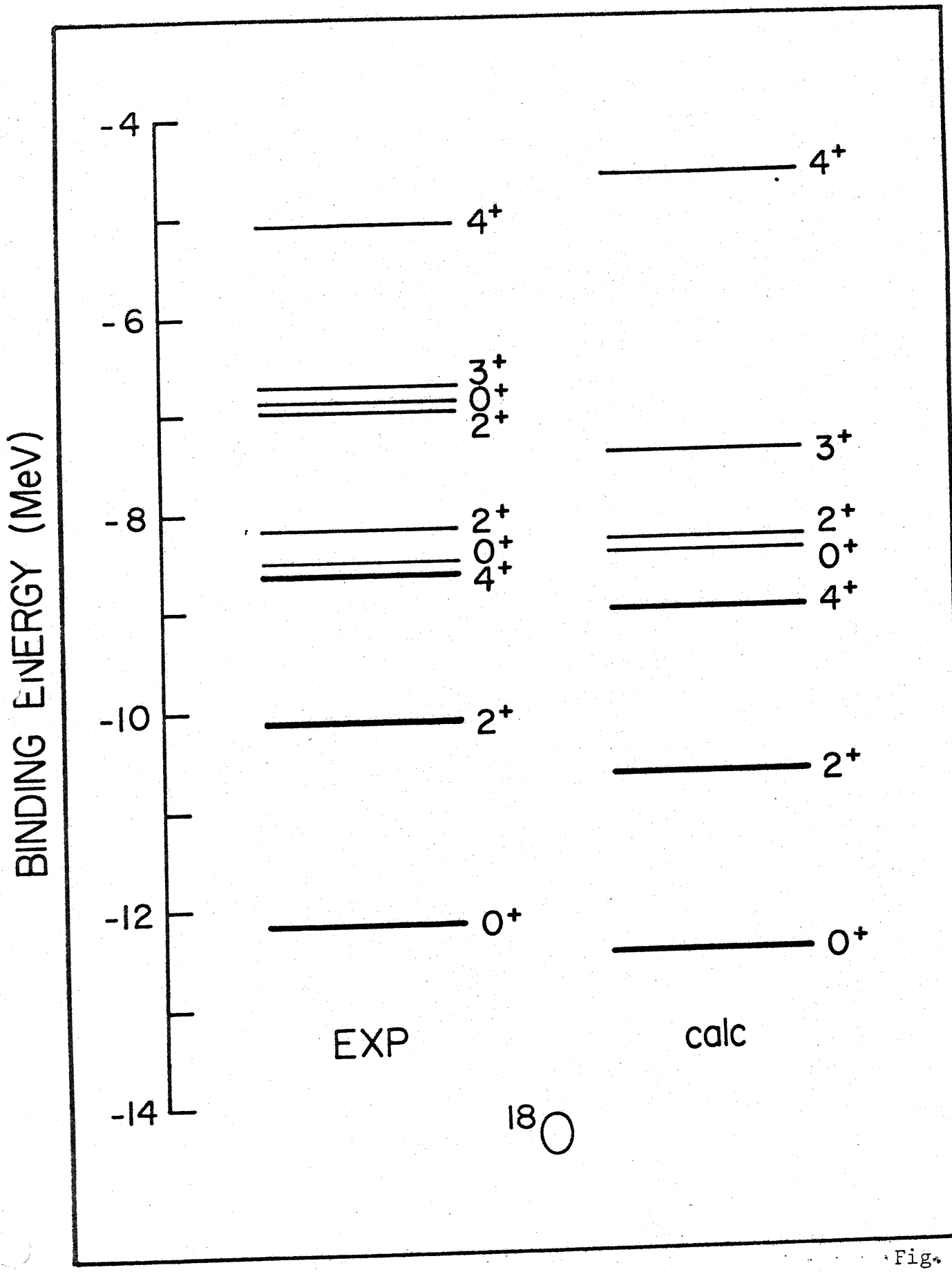
BINDING ENERGY (MeV)
-4
-6
-8
-10
-12
-14
4+
3+
0+
2+
2+
0+
4+
2+
0+
EXP
4+
3+
2+
0+
4+
2+
0+
calc
18O

Fig. 8

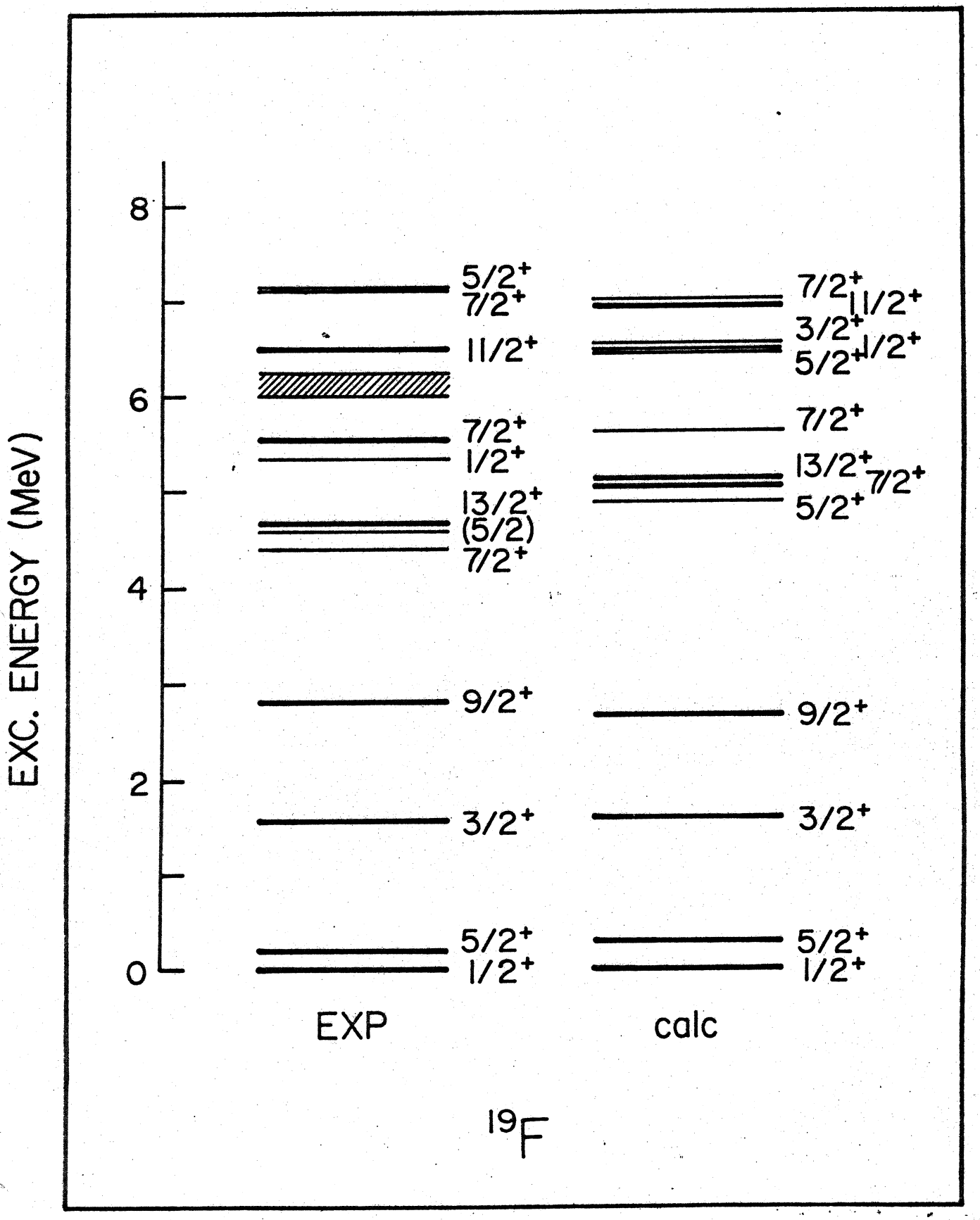
EXC. ENERGY (MeV)
8
6
4
2
0
5/2+
7/2+
11/2+
7/2+
1/2+
13/2+
(5/2)
7/2+
9/2+
3/2+
5/2+
1/2+
EXP
7/2+
11/2+
3/2+
5/2+
1/2+
7/2+
13/2+
7/2+
5/2+
9/2+
3/2+
5/2+
1/2+
calc
19F

Fig. 9

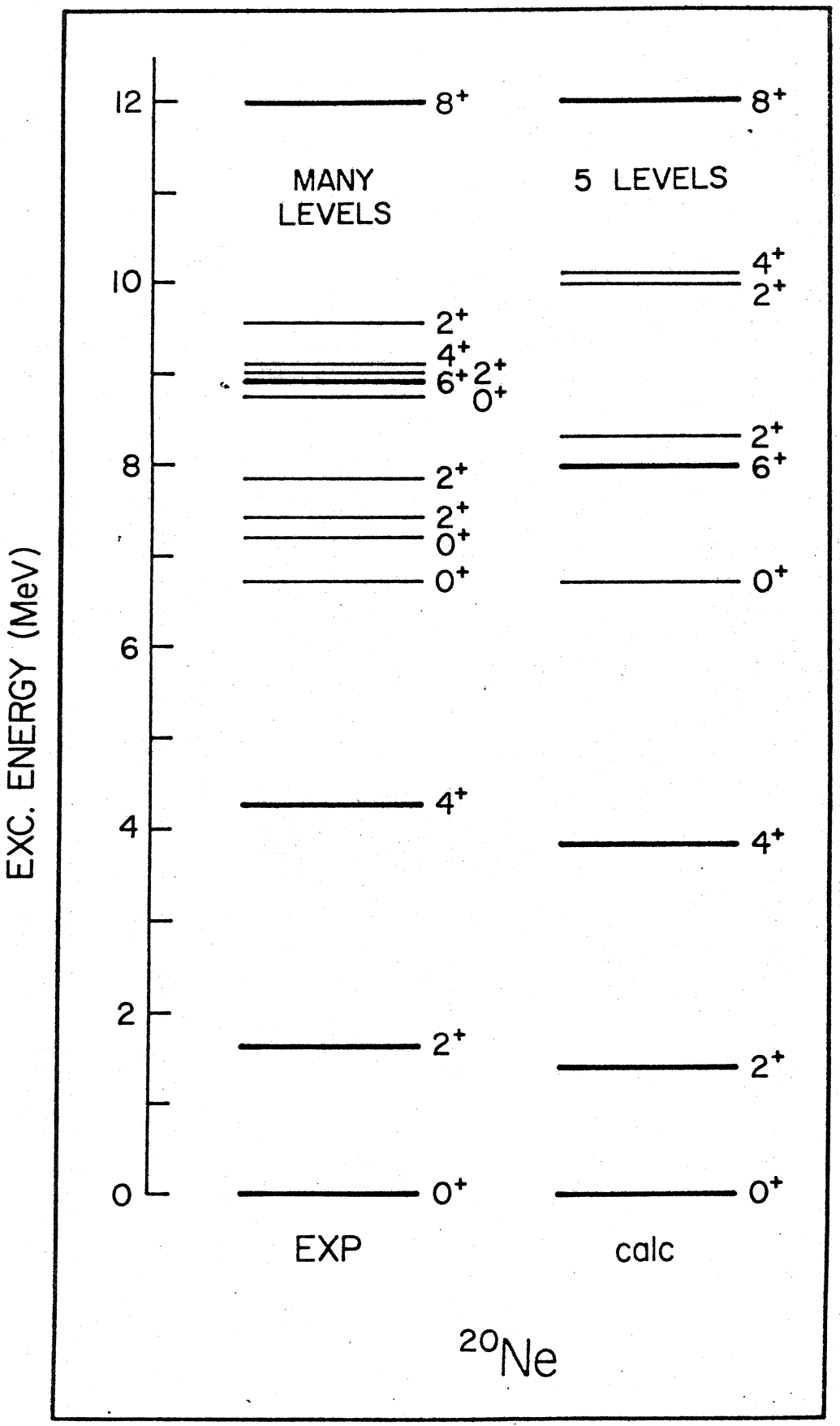
EXC. ENERGY (MeV)
12
10
8
6
4
2
0
MANY LEVELS
5 LEVELS
8+
4+
2+
6+
2+
0+
2+
2+
0+
0+
4+
2+
0+
8+
4+
2+
6+
2+
0+
4+
2+
0+
EXP
calc
20Ne

Fig. 10

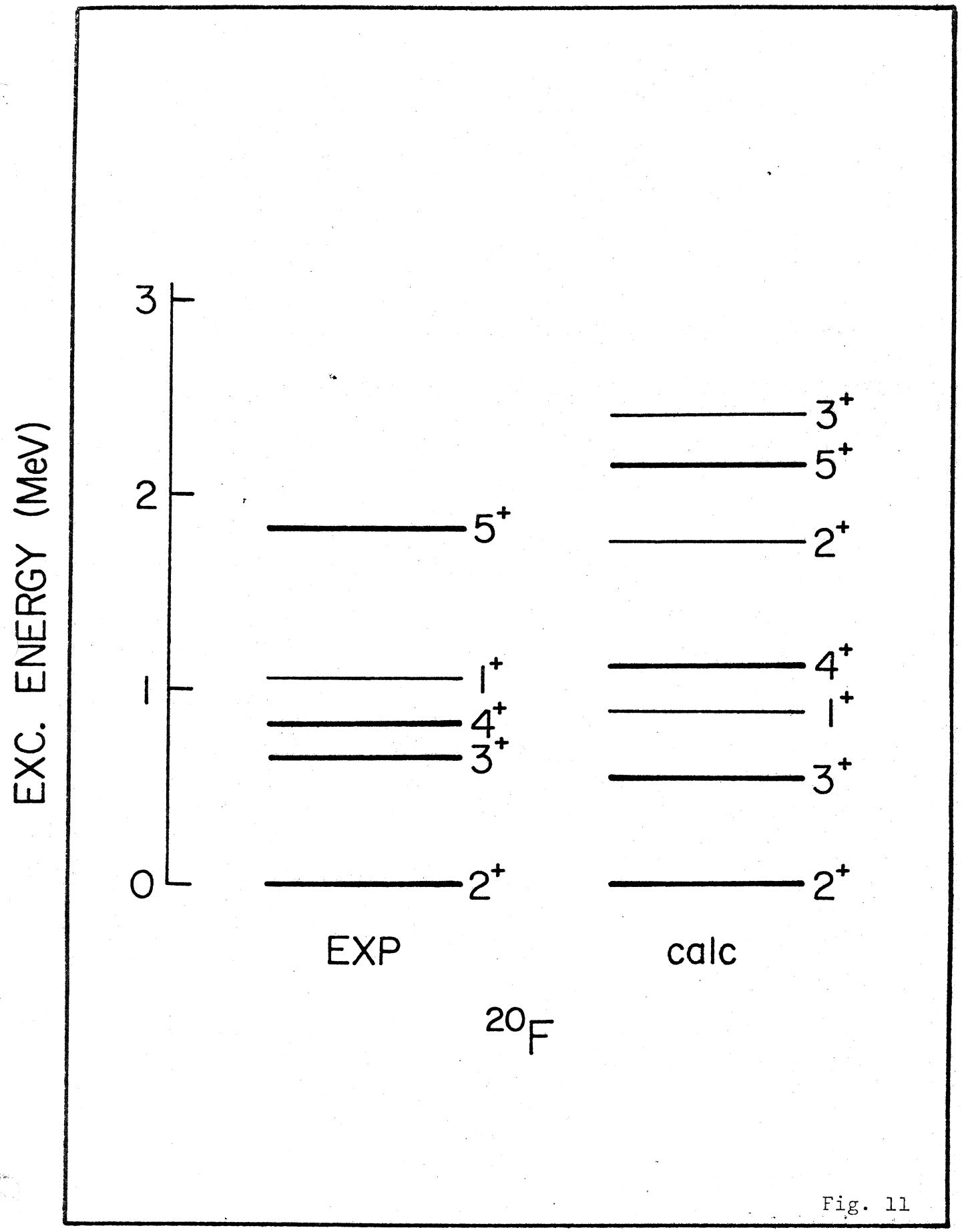

Fig. 11

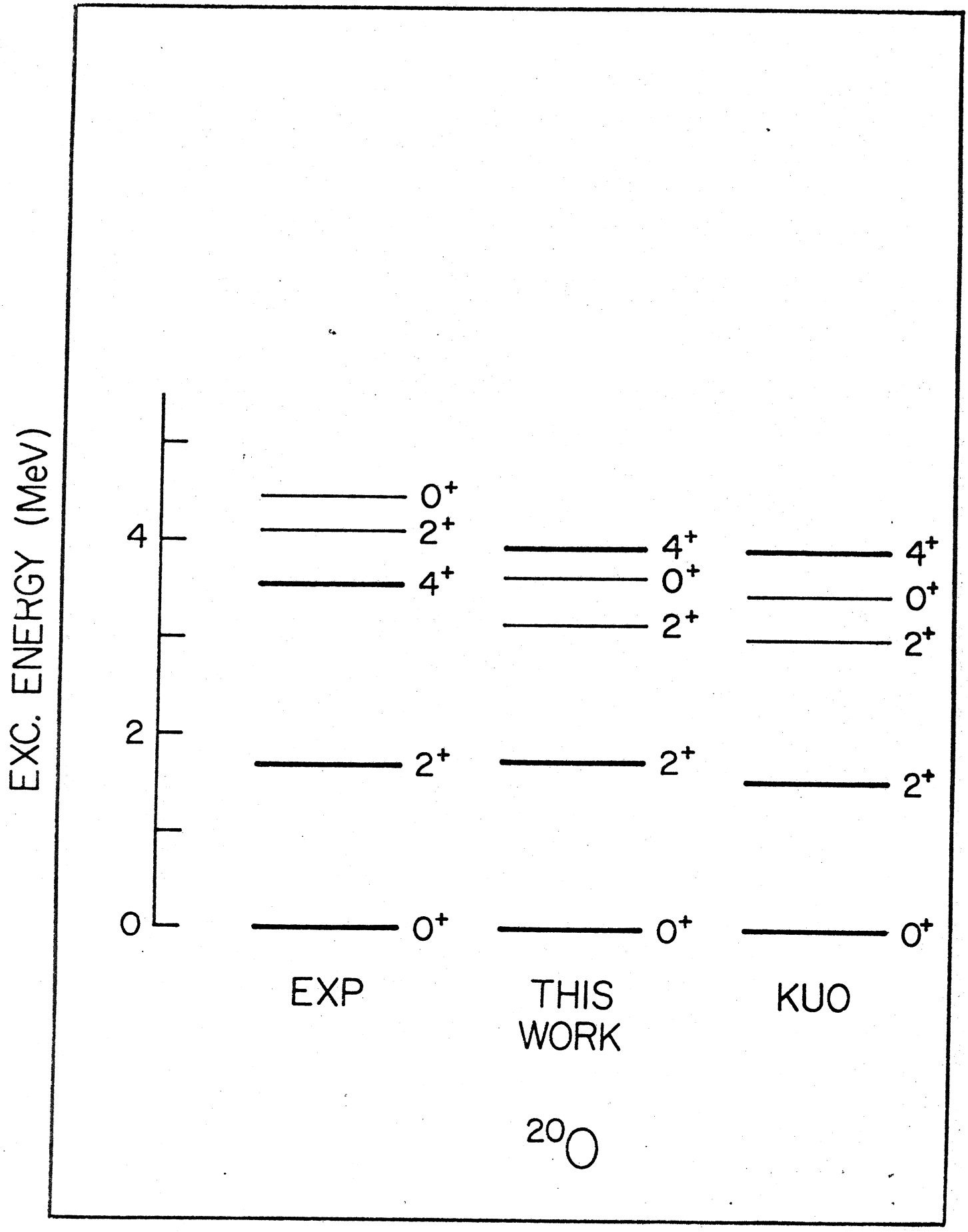

Fig. 12

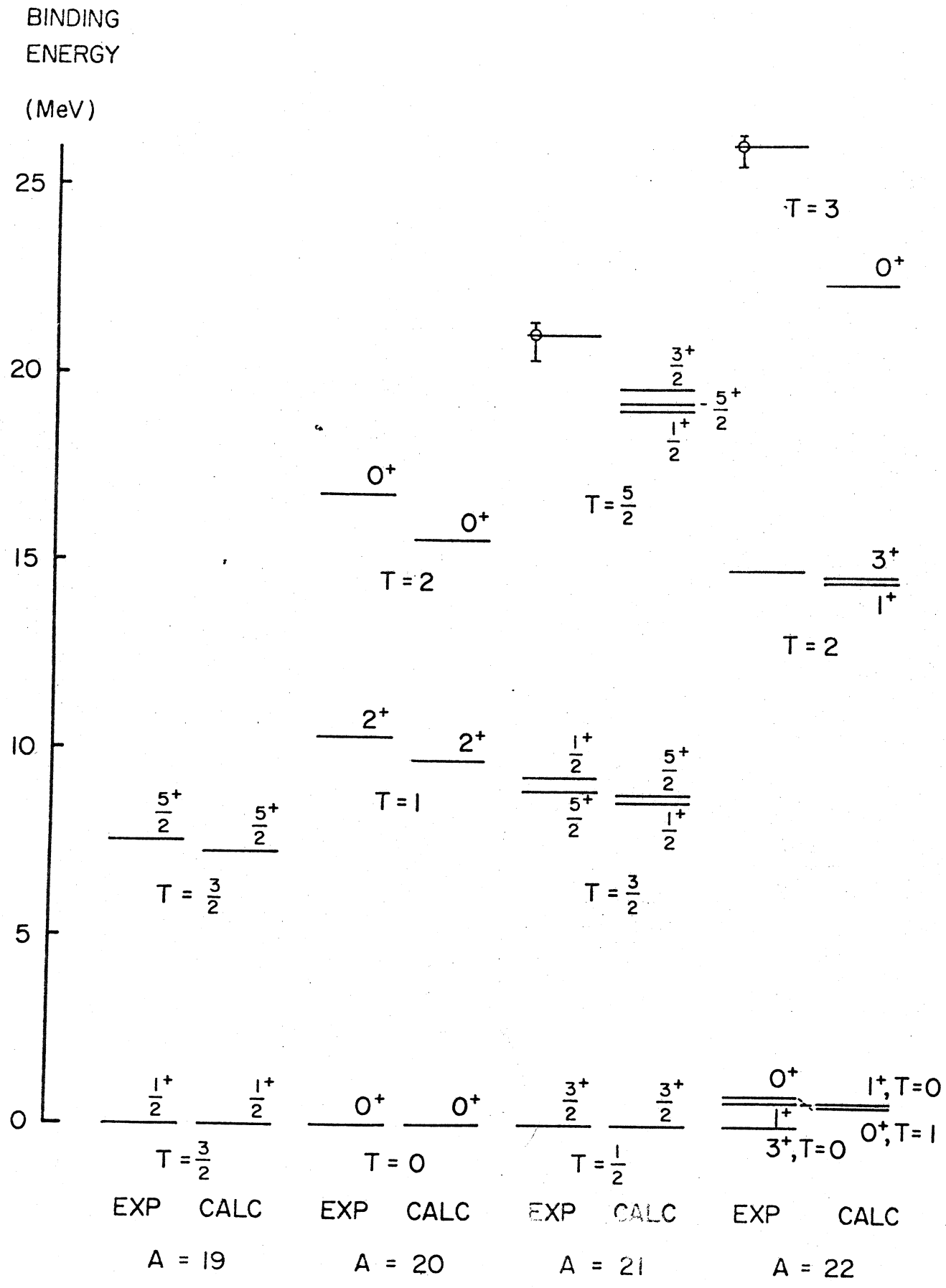
BINDING
ENERGY
(MeV)
25
20
15
10
5
0
T = 3
0+
3+/2
5+/2
1+/2
T = 5/2
0+
0+
T = 2
3+
1+
T = 2
2+
2+
T = 1
1+/2
5+/2
5+/2
1+/2
T = 3/2
5+/2
5+/2
T = 3/2
1+/2
1+/2
T = 3/2
0+
0+
T = 0
3+/2
3+/2
T = 1/2
0+
1+
3+, T=0
1+, T=0
0+, T=1
EXP
CALC
A = 19
EXP
CALC
A = 20
EXP
CALC
A = 21
EXP
CALC
A = 22

Fig. 13

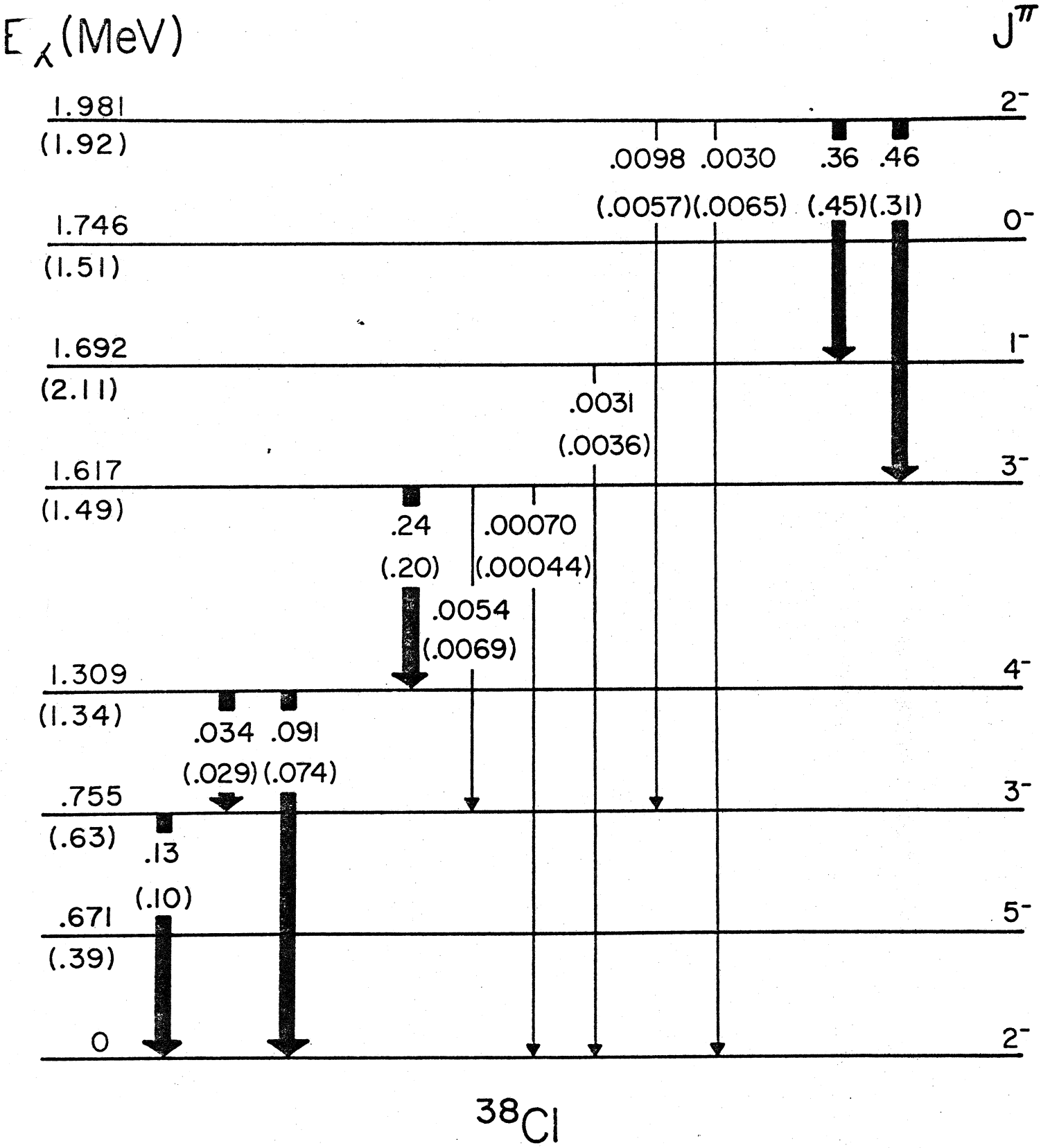
E_x(MeV)
J^π
1.981
(1.92)
2⁻
.0098
.0030
.36
.46
(.0057)
(.0065)
(.45)
(.31)
1.746
(1.51)
0⁻
1.692
(2.11)
1⁻
.0031
(.0036)
1.617
(1.49)
3⁻
.24
(.20)
.00070
(.00044)
.0054
(.0069)
1.309
(1.34)
4⁻
.034
(.029)
.091
(.074)
.755
(.63)
3⁻
.13
(.10)
.671
(.39)
5⁻
0
2⁻
^{38}Cl

Fig. 14.

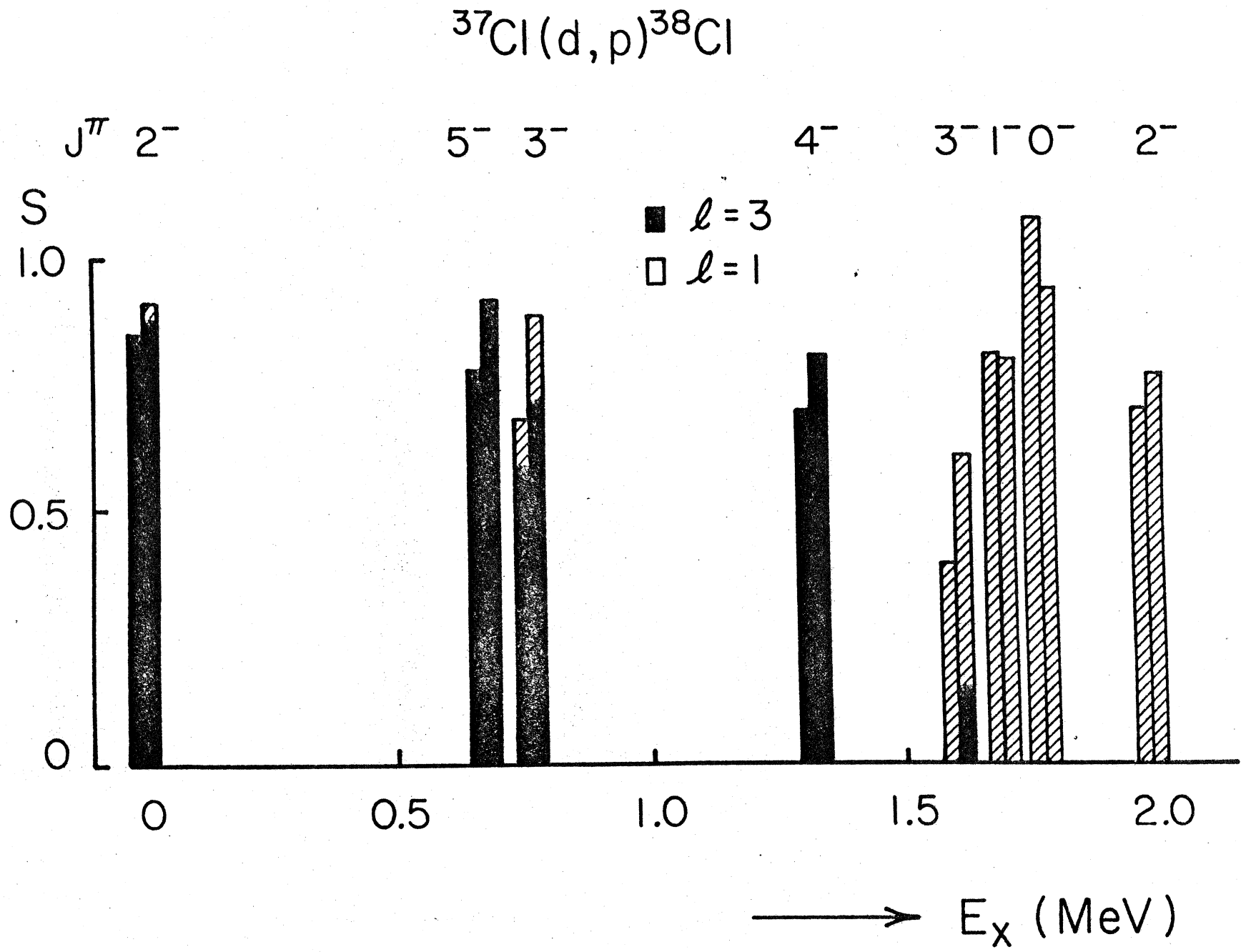

Fig. 15